COBEM 2023 27TH INTERNATIONAL CONGRESS OF MECHANICAL ENGENEERING

ABCM Brazilian Society of Mechanical Sciences and Engineering
27th ABCM International Congress of Mechanical Engineering
December 04-08, 2023, Florianópolis-SC, Brazil

COBEM2023-0750
Comparison between Pseudopotential and Phase-field Lattice Boltzmann Method for the liquid-gas phase-change Stefan Problem

Ivan Talão Martins
Department of Mechanical Engineering, Heat Transfer Research Group, São Carlos School of Engineering (EESC), University of São Paulo (USP), São Carlos, 13566-590, São Paulo, Brazil.
ivanmartins@usp.br

Alfredo Jaramillo Palma
Center of Innovation for Flow through Porous Media, University of Wyoming, Laramie, United States.
alfredo.jaramillo@uwyo.edu

Luben Cabezas-Gómez
Department of Mechanical Engineering, Heat Transfer Research Group, São Carlos School of Engineering (EESC), University of São Paulo (USP), São Carlos, 13566-590, São Paulo, Brazil.
lubencg@sc.usp.br

Abstract. *The lattice Boltzmann method (LBM) is a mesoscale numerical method that has been largely applied for simulating multiphase and multicomponent flows, giving its facility for considering the interaction between different phases and components. Many multiphase LBM models can be found in the literature. Assessing the limitations of those models is of high relevance as it allows to select the strategy with the best balance between accuracy and computational performance for each application. Because of this, the present work compares two multiphase LBM widely used in the literature: 1) the pseudopotential LBM, and 2) the Cahn-Hilliard-based phase-field LBM. The simulations performed correspond to a 1D liquid-gas phase change problem (the Stefan problem) ranging across three reduced temperatures (0.97, 0.86 and 0.76), and two working fluids (water and R134a). In comparison with the analytical solution, the results show that the pseudopotential LBM can capture the liquid-gas interface advance correctly only for the higher reduced temperature (TR = 0.97), presenting unsatisfactory results for others TRs. On the other hand, the phase-field LBM was able to capture the interface advance for the three simulated TRs with good accuracy. However, due to stability issues, for this latter model it was necessary to adopt low values of Δt and Δx, decreasing the overall computational efficiency of the model.*

Keywords: *Liquid-gas phase-change simulation, phase-field lattice Boltzmann method, Pseudopotential lattice Boltzmann method, Cahn-Hilliard equation.*

1. INTRODUCTION

The liquid-gas phase-change phenomenon has attracted a lot of attention in the last decade (Carey, 2020). Giving its power for energy transferring, it can be used as an efficient heat transfer mechanism for refrigerating systems, particularly when the size of the refrigeration devices is small, having to dissipate more heat power in less area. Thus, the study of vaporization processes is of great importance for understanding liquid-gas phase-change, as well as for the development of refrigeration systems.

There are several possible approaches for the study of boiling phenomena, including experimental observations, theoretical formulations and numerical analysis (Zuber, 1959; Son *et al.*, 2002). This paper focuses in the last kind of study. Many numerical methods for multi-phase flows were developed over last decades, being the most famous the Level Set method (Osher and Sethian, 1988; Fedkiw, 2003) and the Volume of Fluid - VOF method (Hirt and Nichols, 1981; Ferrari and Lunati, 2013). However, the consideration of phase-separation, and the interface dynamics represent cumbersome challenges for these traditional methods, particularly in fluid-solid interactions Liu *et al.* (2016).

The lattice Boltzmann method (LBM) is a mesoscopic numerical method based on the discretization of the Boltzmann transport equation which was developed in the second half of the 20th century from the Lattice Cellular Automata method. The mesoscale nature of the LBM allows the consideration of necessary properties and physical phenomena to treat multiphase flows in a natural way, like by means of intermolecular forces, or by means of potentials tailored from the system's free energy (Premnath *et al.*, 2005). Consequently, the LBM is an attractive numerical alternative to traditional methods when dealing with liquid-gas phase-change problems.

In the last three decades, several LBM models for multiphase flows were developed, such as the color-gradient method

(Gunstensen *et al.*, 1991), the free-energy-based models (Swift *et al.*, 1996), the pseudopotential method (Shan and Chen, 1993), and the phase-field-based models (He *et al.*, 1999). Therefore, it is important to evaluate the limitations and advantages of each model in relation to the others.

In this paper, we present the comparison between the performance of the pseudopotential LBM model proposed by Li *et al.* (2013) and the phase-field-based LBM model proposed by Lee and Liu (2010) with the modifications proposed by Safari *et al.* (2013) to consider phase-change. The Stefan problem was considered for this analysis, along with two fluids (water, and R134a) at three reduced temperatures (0.97, 0.86, and 0.76). The numerical results were compared with the analytical solution for evaluating the accuracy of each method.

2. METHODOLOGY

In this section, we present a brief description of each LBM model considered in this work.

2.1 Pseudopotential Lattice Boltzmann Method

The pseudopotential method bases on the addition of forcing terms in the traditional LBE in order to mimic the interaction between the particles of the fluid (and eventually, between fluid-solid particles). The traditional LBE for a generic collision matrix Λ_{ij} with a forcing scheme similar to the proposed by Guo *et al.* (2002) can be given by the following equation (Krüger *et al.*, 2017),

$$f_i(\mathbf{x}+\mathbf{e}_i\Delta t, t+\Delta t) - f_i(\mathbf{x},t) = -\Delta t \left[\mathbf{M}^{-1}\mathbf{\Lambda}\mathbf{M}\right]_{ij}\left[f_j - f_j^{eq}\right]_{(\mathbf{x},t)} + \Delta t M_{ij}^{-1}\left(I_{ij} - \frac{\Delta t \Lambda_{ij}}{2}\right) S_j|_{(\mathbf{x},t)}, \quad (1)$$

where I_{ij} is the identity matrix.

The macroscopic variables such as density and *momentum* are given by the moments of the distribution functions f_i:

$$\rho(\mathbf{x},t) = \sum_i f_i(\mathbf{x},t), \quad (2)$$

$$\rho\mathbf{u}(\mathbf{x},t) = \sum_i \mathbf{e}_i f_i(\mathbf{x},t) + \frac{\Delta t}{2}\mathbf{F}(\mathbf{x},t)\ , \quad (3)$$

where $\mathbf{F}$ denote the forces acting on the fluid. Also, the equilibrium distribution functions are defined by

$$f_i^{eq}(\mathbf{x},t) = \rho(\mathbf{x},t)\omega_i\left[1 + \frac{\mathbf{e}_i\cdot\mathbf{u}(\mathbf{x},t)}{c_s^2} + \frac{(\mathbf{e}_i\cdot\mathbf{u}(\mathbf{x},t))^2}{2c_s^4} - \frac{\mathbf{u}(\mathbf{x},t)\cdot\mathbf{u}(\mathbf{x},t)}{2c_s^2}\right]\ , \quad (4)$$

where c_s the sound speed, ω_i the lattice weights and $\mathbf{e}_i$ the discrete particle velocities, which depends of the velocity scheme chosen (Qian *et al.*, 1992).

Over the years many collision schemes have been developed. One of them is the BGK collision operator (Bhatnagar *et al.*, 1954), which assumes that the collision matrix Λ_{ij} is a diagonal matrix with all its diagonal elements equal to $1/\tau$, where τ is a time relaxation parameter. Emplyoing the Chapman-Enskog analysis (Chapman and Cowling, 1952), it is possible to relate this time relaxation parameter with the fluid kinematic viscosity as $\nu = (\tau - \Delta t/2)c_s^2$.

However, this linear collision operator can be more prone to unstable behavior. The Multiple-relaxation-time (MRT) collision operator can be utilized to overcome this issue. First, the collision process is transformed to the momentum space multiplying Eq. (1) by the transformation matrix $\mathbf{M}$ (see Krüger *et al.* (2017)). The collision matrix for the MRT is defined also as a diagonal matrix with each element of the main diagonal related to one moment of the distribution function. For example, for the D2Q9 velocity scheme: $\Lambda_{ij} - \text{diag}(\tau_\rho^{-1}, \tau_e^{-1}, \tau_\zeta^{-1}, \tau_j^{-1}, \tau_q^{-1}, \tau_j^{-1}, \tau_q^{-1}, \tau_\nu^{-1}, \tau_\nu^{-1})$. After processing the collision process, the post-collision distribution functions f_i^* can be obtained by multiplying the post-collision moments $\mathbf{m}^*$ by the inverse of the transformation matrix ($\mathbf{f}^* = \mathbf{M}^{-1}\cdot\mathbf{m}^*$).

The interaction force $\mathbf{F_m}$ is the key concept used by the pseudopotential LBM to deal with the phase-change process, representing the interaction forces between the molecules of the fluid. Following Chen and Doolen (1998), this force can be defined by Eq. (5). In that equation, w_i are weights defined as $w_i = 1/3$ if $|\mathbf{e}_i|^2 = 1$ and $w_i = 1/12$ if $|\mathbf{e}_i|^2 = 2$ (Sbragaglia *et al.*, 2007). Also $\psi(\mathbf{x},t)$ is the pseudopotential field, and G corresponds to the interaction strength.

$$\mathbf{F_m}(\mathbf{x},t) = -G\psi(\mathbf{x},t)\sum_i w_i\psi(\mathbf{x}+\mathbf{e}_i\Delta t,t)\mathbf{e}_i \quad (5)$$

The pseudopotential term can be defined as a function of the thermodynamic pressure from a non-ideal equation of state (EOS), as indicated in Eq. (6). With this equation, G no longer stands for the intermolecular strength, being used only to guarantee a positive value inside the square root. The value $G = -1$ was adopted in this work.

$$\psi(\mathbf{x},t) = \sqrt{\frac{2\left[p_{EOS}(\mathbf{x},t) - \rho(\mathbf{x},t)/3\right]}{G}} \tag{6}$$

The thermodynamic pressure is modeled in terms of the Peng-Robinson EOS (7), where T_c is the critical temperature, γ is the acentric factor, R is the universal gas constant, $a = 0.45724R\,2T_c^2/p_c$, $b = 0.0778RT_c/p_c$, and p_c is the pressure at the critical point.

$$p_{EOS}(\mathbf{x},t) = \frac{\rho(\mathbf{x},t)RT(\mathbf{x},t)}{1-b\rho(\mathbf{x},t)} - \frac{1+\left(0.37464+4.54226\gamma-0.2699\gamma^2\right)\left(1-\sqrt{T(\mathbf{x},t)/T_c}\right)}{1-2b\rho(\mathbf{x},t)-b^2\rho(\mathbf{x},t)^2} \tag{7}$$

The forcing term S_i is defined defined as (Jaramillo *et al.*, 2022):

$$\mathbf{S} = \begin{bmatrix} 0 \\ 6\left(\mathbf{u}\cdot\mathbf{F}\right) + \frac{12\sigma(\mathbf{F_m}\cdot\mathbf{F_m})^2}{\psi^2(\tau_e-\Delta t/2)} \\ -6\left(\mathbf{u}\cdot\mathbf{F}\right) - \frac{12\sigma(\mathbf{F_m}\cdot\mathbf{F_m})^2}{\psi^2(\tau_\zeta-\Delta t/2)} \\ F_x \\ -F_x \\ F_y \\ -F_y \\ 2(u_xF_x - u_yF_y) \\ u_xF_y + u_yF_x \end{bmatrix}. \tag{8}$$

The subscripts x and y indicate the coordinate directions of $\mathbf{F}$ and $\mathbf{u}$. The parameter σ is used in the forcing term to adjust the thermodynamic consistency of the pseudopotential model (Lycett-Brown and Luo, 2015). A correction term $\mathbf{C} = \mathbf{M}^{-1}\left[0, 1.5\tau_e^{-1}\left(Q_{xx}+Q_{yy}\right), -1.5\tau_\zeta^{-1}\left(Q_{xx}+Q_{yy}\right), 0, 0, 0, -\tau_\nu^{-1}(Q_{xx}-Q_{yy}), -\tau_\nu^{-1}Q_{xy}\right]$ is added to Eq. (1) to tune the surface tension in the LBM model, guarantying its value matches the surface tension of the simulated fluid (Jaramillo *et al.*, 2022). In this additional term, $\mathbf{Q}$ is defined as $\mathbf{Q} = \kappa\frac{G}{2}\psi(\mathbf{x},t)\sum_i w_i\left[\psi(\mathbf{x}+\mathbf{e}_i\Delta t,t)-\psi(\mathbf{x},t)\right]\mathbf{e}_i\mathbf{e}_i$, where κ is the tuning parameter.

In the simulations considered in this work, a two-dimensional domain was setup by utilizing the D2Q9 scheme. To preserve the symmetry of the problem, the top and bottom boundaries were considered adiabatic rigid walls. For more details about the pseudopotential model used in the simulations the interested reader is referred to Jaramillo *et al.* (2022).

2.2 Cahn-Hilliard-based Lattice Boltzmann Method

The phase-field model considered in this work corresponds to the multi-phase LBM developed by Lee and Liu (2010), with the modification proposed by Safari *et al.* (2013) for the consideration of the phase-change process. Defining ϕ as the phase concentration, it is assumed that $\phi = 1.0$ for the liquid phase, and $\phi = 0.0$ for the gas one. Then, the LBE for recovering the Cahn-Hilliard equation can be defined as follows,

$$\begin{aligned} h_i(\mathbf{x}+\mathbf{e}_i\Delta t, t+\Delta t) - h_i(\mathbf{x},t) = &-\frac{\Delta t}{\tau}\left[h_i - h_i^{eq}\right]_{(\mathbf{x},t)} + ... \\ &\Delta t\left(\mathbf{e}_i-\mathbf{u}\right)\cdot\left[\nabla^{MD}\phi - \frac{\phi}{\rho c_s^2}\left(\nabla^{MD}p + \phi\nabla^{MD}\mu\right)\right]_{(\mathbf{x},t)} + ... \\ &\frac{\Delta t}{2}\left(M\Gamma_i\nabla^2\mu - \frac{\dot{m}'''}{\rho_l}\right)_{(\mathbf{x},t)} + \frac{\Delta t}{2}\left(M\Gamma_i\nabla^2\mu - \frac{\dot{m}'''}{\rho_l}\right)_{(\mathbf{x}+\mathbf{e}_i\Delta t,t)}, \end{aligned} \tag{9}$$

being $p(\mathbf{x},t)$ the hydrodynamic pressure of the system, $\rho(\mathbf{x},t)$ the local density, M the mobility, μ the chemical potential, and $\dot{m}'''$ the volumetric source of vapor mass. The parameter Γ_i is defined as $\Gamma_i = \omega_i\left[1+\frac{\mathbf{e}_i\cdot\mathbf{u}}{c_s^2}+\frac{(\mathbf{e}_i\cdot\mathbf{u})^2}{2c_s^4}-\frac{\mathbf{u}\cdot\mathbf{u}}{2c_s^2}\right]_{(\mathbf{x},t)}$. The equilibrium distribution functions are defined as Eq. (10).

$$h_i^{eq}(\mathbf{x},t) = \omega_i\phi\left[1+\frac{\mathbf{e}_i\cdot\mathbf{u}}{c_s^2}+\frac{(\mathbf{e}_i\cdot\mathbf{u})^2}{2c_s^4}-\frac{\mathbf{u}\cdot\mathbf{u}}{2c_s^2}\right]_{(\mathbf{x},t)} - \frac{\Delta t}{2}\left(\mathbf{e}_i-\mathbf{u}\right)\cdot\left[\nabla^{CD}\phi - \frac{\phi}{\rho c_s^2}\left(\nabla^{CD}p+\phi\nabla^{CD}\mu\right)\right]_{(\mathbf{x},t)} \tag{10}$$

The macroscopic liquid concentration ϕ can be recovered from the distribution functions h_i by its zero-order moment as:

$$\phi(\mathbf{x},t) = \sum_i h_i(\mathbf{x},t). \tag{11}$$

The density field can be calculated as a linear function of the concentration: $\rho(\mathbf{x},t) = \phi(\mathbf{x},t)\rho_l + (1-\phi(\mathbf{x},t))\rho_v$. For the fluid *momentum* conservation equation, the LBE with the BGK collision operator can be defined by Eq. (12).

$$\begin{aligned} g_i(\mathbf{x}+\mathbf{e}_i\Delta t, t+\Delta t) - g_i(\mathbf{x},t) = -\frac{\Delta t}{\tau}\left[g_i - g_i^{eq}\right]_{(\mathbf{x},t)} + ... \\ \Delta t\left(\mathbf{e}_i - \mathbf{u}\right)\cdot\left[\nabla^{MD}\rho c_s^2\left(\Gamma_i - \Gamma_i(\mathbf{0})\right) - \phi\nabla^{MD}\mu\Gamma_i\right]_{(\mathbf{x},t)} + ... \\ \frac{\Delta t}{2}\rho c_s^2\dot{m}'''\left(\frac{1}{\rho_v}-\frac{1}{\rho_l}\right)\Gamma_i(\mathbf{0})|_{(\mathbf{x},t)} + \frac{\Delta t}{2}\rho c_s^2\dot{m}'''\left(\frac{1}{\rho_v}-\frac{1}{\rho_l}\right)\Gamma_i(\mathbf{0})|_{(\mathbf{x}+\mathbf{e}_i\Delta t,t)} \end{aligned} \tag{12}$$

The equilibrium distribution function for the pressure distribution functions g_i can be defined as,

$$\begin{aligned} g_i^{eq}(\mathbf{x},t) = \omega_i\left\{p + \rho c_s^2\left[\frac{\mathbf{e}_i\cdot\mathbf{u}}{c_s^2} + \frac{(\mathbf{e}_i\cdot\mathbf{u})^2}{2c_s^4} - \frac{\mathbf{u}\cdot\mathbf{u}}{2c_s^2}\right]\right\}_{(\mathbf{x},t)} - ... \\ \frac{\Delta t}{2}\left(\mathbf{e}_i - \mathbf{u}\right)\cdot\left[\nabla^{CD}\rho c_s^2\left(\Gamma_i - \Gamma_i(\mathbf{0})\right) - \phi\Gamma_i\nabla^{CD}\mu\right]_{(\mathbf{x},t)}. \end{aligned} \tag{13}$$

The macroscopic pressure and *momentum* of the fluid are recovered by the moments of the distribution function as:

$$p(\mathbf{x},t) = \sum_i g_i(\mathbf{x},t) + \frac{\Delta t}{2}\mathbf{u}\cdot\nabla^{CD}\rho c_s^2, \tag{14}$$

$$\rho\mathbf{u}(\mathbf{x},t) = \frac{1}{c_s^2}\sum_i \mathbf{e}_i g_i(\mathbf{x},t) - \frac{\Delta t}{2}\phi\nabla^{CD}\mu. \tag{15}$$

Considering the BGK collision operator, it is possible to recover the conservation laws (mass and *momentum*) from the LBE by employing the Chapman-Enskog analysis. Doing so, the relaxation can be related to the kinematic viscosity of the fluid as $\nu = (\tau - \Delta t/2)\, c_s^2$.

The spatial derivatives ∇^{CD} (central difference), ∇^{MD} (mixed difference), and ∇^2 are calculated in the same way as suggested by Lee and Liu (2010).

The chemical potential can be calculated from the free energy function as $\mu = \partial_\phi\psi - \kappa\nabla^2\phi$ (Bray, 1994), being ψ the volumetric free energy. In the neighborhood of the critical point, a simplification for the volumetric free energy can be adopted: $\psi(\phi) = \beta\phi^2(1-\phi)^2$ (Rowlinson and Widom, 1982). Although this approach assumes that the fluid is isotherm, it is still a reasonable approach when considering heat transfer problems, as it will be verified by the results in this paper.

The final expression for the chemical potential is: $\mu = 4\beta\phi(\phi-1)(\phi-1/2) - \kappa\nabla^2\phi$. The constants β and κ are related with the surface tension of the fluid σ and the interface width W as $\kappa = \frac{3}{2}\sigma W$ and $\beta = \frac{12\sigma}{W}$. Because the model is based on the consideration of a diffuse interface between the fluid phases, in all the simulations of this paper we assumed an interface width of $W = 5\Delta x$.

The volumetric mass source of vapor is derived assuming that all the heat transferred do the liquid-gas interface is consumed for vapor generation. Then according to Safari *et al.* (2013),

$$\dot{m}''' = \frac{k_g\nabla^{CD}T}{h_{lv}}\cdot\nabla^{CD}\phi. \tag{16}$$

For this method, D1Q3 velocity scheme was adopted in the simulations, along with the wet-node boundary approach.

2.3 Thermal Lattice Boltzmann Method

The two population model was adopted in order to model energy transfer, such model considers an additional distribution function s_i for the thermal energy propagation. Neglecting the viscous dissipation and compression work, and considering incompressible flows and constant fluid properties (density, specific heat and conductivity), the LBE with the BGK collision operator for the energy equation can be expressed as (Krüger *et al.*, 2017):

$$s_i(\mathbf{x}+\mathbf{e}_i\Delta t, t+\Delta t) - s_i(\mathbf{x},t) = -\frac{\Delta t}{\tau_s}\left[s_i(\mathbf{x},t) - s_i^{eq}(\mathbf{x},t)\right]. \tag{17}$$

And the following linear equilibrium distribution function was considered:

$$s_i^{eq}(\mathbf{x},t) = \omega_i T(\mathbf{x},t)\left[1 + \frac{\mathbf{e}_i\cdot\mathbf{u}(\mathbf{x},t)}{c_s^2}\right]. \tag{18}$$

Then, the temperature distribution on the domain can be recovered according to:

$$T(\mathbf{x},t) = \sum_i s_i(\mathbf{x},t) \tag{19}$$

The relaxation time is related with the thermal diffusivity of the domain by the relation $\alpha = (\tau_s - \Delta t/2)\, c_s^2$.

For one-dimensional simulations with *wet-node* boundary scheme, the Dirichlet's boundary conditions can be implemented as suggested by Mohamad (2019). For example. considering a fixed temperature T_w, the unknown function at the boundary node $\mathbf{x}_w$, indicated by the label "unk", can be calculated as $s_{i_{unk}}(\mathbf{x}_w,t) = T_w - \sum_{i\neq i_{unk}} s_i(\mathbf{x}_w,t)$.

3. RESULTS

The main goal of this paper is the comparison between the performance of two lattice Boltzmann models for liquid-gas phase-change problems: the pseudopotential model and the Cahn-Hilliard-based model proposed by Lee and Liu (2010). Then, similar to Welch and Wilson (2000) a simple vaporization problem with analytical solution was selected as test for this comparison: the Stefan problem. The existence of an analytical solution allows for a better analysis of the results provided by each method, favoring a quantitative comparison of the results.

3.1 The Stefan Problem

The Stefan problem consists in a resting saturated liquid in contact with a super-heated wall with constant temperature T_w at the left boundary. The excess of energy coming from this boundary triggers the vaporization of the liquid, since $T_w > T_{sat}$ (being T_{sat} the saturation temperature of the fluid). As the emerging gas phase transfers the heat to the liquid-gas interface, more vapor is generated and the interface advances towards the liquid region. Fig. 1 shows a scheme of this physical setting.

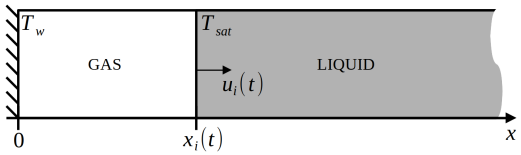

Figure 1: Ilustration of the Stefan problem for a liquid-gas interface.

Both phases are assumed to be incompressible, and the liquid is assumed to remain at saturation temperature, meaning that all the heat transferred by the gas phase is consumed in the vaporization process (Stefan boundary). Thus, there is only heat diffusion in the vapor. Considering a one-dimensional formulation, the mathematical equations that model the problem are presented in Eq. (20), being ρ the density, k the thermal conductivity, α the thermal diffusivity and h_{lv} the latent heat of vaporization. The subscript v indicates the properties for the vapor phase.

$$\begin{cases} \partial_t T = \alpha_v \partial_{xx} T, \text{ if } 0 \le x \le x_i(t) \\ T(0,t) = T_w \\ T(x_i(t),t) = T_{sat} \\ \rho_v u_i(t) h_{lv} = -k_v \partial_x T|_{x_i(t)} \end{cases} \tag{20}$$

From this set of equations it is possible to obtain a solution for the interface position in time, $x_i(t)$, as well as its velocity, $u_i(t)$. This solution is given by (Hahn and Özişik, 2012):

$$x_i(t) = 2\lambda\left(\alpha_g t\right)^{1/2}, \tag{21}$$

being λ a constant determined by the transcendental Eq. (22), with $c_{p,g}$ being the specific heat of the gas at constant pressure. The interface velocity can be obtained from Eq. (21), and it reads $u_i(t) = \partial_t x_i(t) = \lambda\left(\alpha_v t^{-1}\right)^{1/2}$.

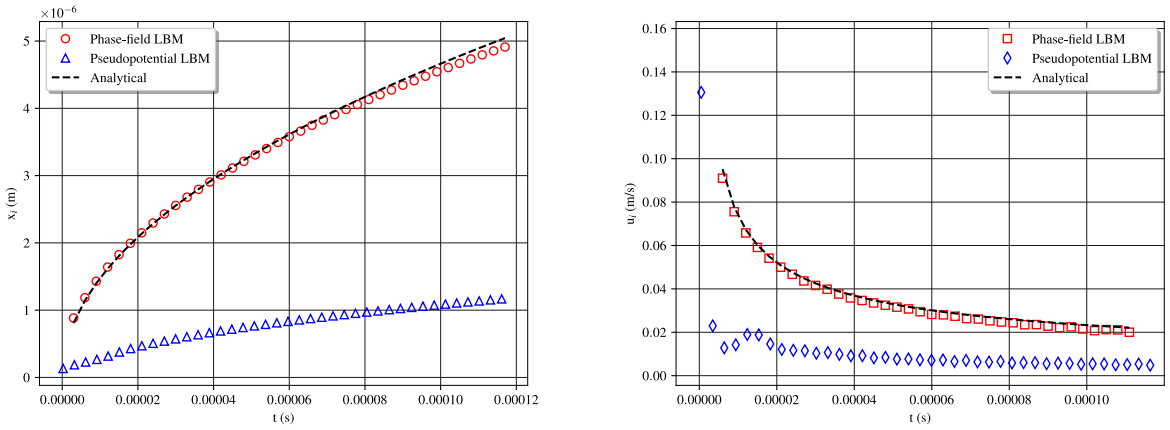

(a) (b)

Figure 2: Interface position (a) and velocity (b) for saturated water, considering $T_r = 0.76$.

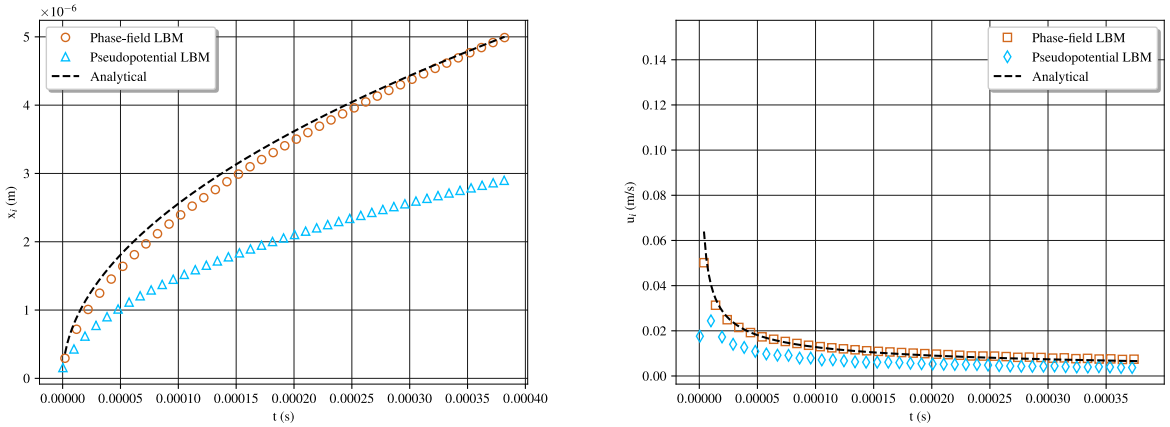

(a) (b)

Figure 3: Interface position (a) and velocity (b) for saturated water, considering $T_r = 0.86$.

$$\lambda e^{\lambda^2} \mathrm{erf}(\lambda) = \frac{c_{p,g}\left(T_w - T_{sat}\right)}{h_{lv}\sqrt{\pi}} = \frac{S_t}{\sqrt{\pi}}\,, \tag{22}$$

where $S_t = c_{p,g}\left(T_w - T_{sat}\right)/h_{lv}$ is the Stefan number.

3.2 Numerical Solutions and Discussion

The properties of water and R134a, such as ρ, c_p, k, h_{lv}, σ (surface tension), and ν (kinematic viscosity), were taken from the CoolProp library (Bell *et al.*, 2014). The wall temperature T_w was assumed in such a way to configure a Stefan number about $S_t = 0.1$ for all the simulations. The same temporal and spatial discretization were used for both LBM models: $\Delta t = 3.0 \cdot 10^{-11}$s and $\Delta x = 5.0 \cdot 10^{-8}$m. The simulations stop at the time for which the analytical solution for the liquid-gas interface position reaches 5.0 μm. Then, the real time simulated can be expressed as:

$$t_{stop} = \left(\frac{5 \cdot 10^{-6}}{2\lambda}\right)^2 \alpha_v^{-1}\,.$$

The left boundary was considered as a stationary wall modeled by the bounce-back rule for f_i, g_i and h_i (see Guo and Shu (2013)). The right boundary was considered an open outlet, implemented by the first order extrapolation method, see Mohamad (2019). For the thermal related LBM, according to the Stefan Problem described in Sec. 3.1, the left boundary remains at a constant temperature, implemented as mentioned in sec. 2.3 Whereas for the right boundary a first order extrapolation method employed.

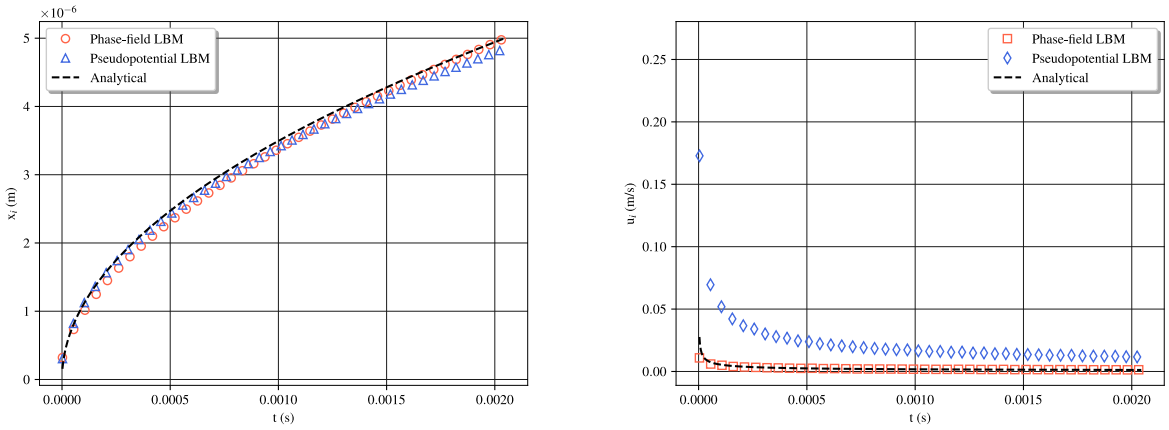

(a) (b)

Figure 4: Interface position (a) and velocity (b) for saturated water, considering $T_r = 0.97$.

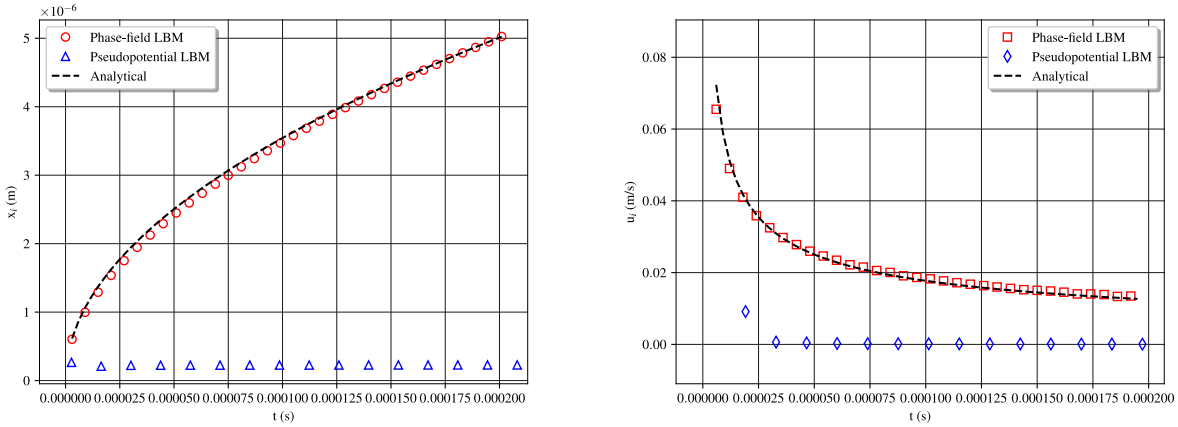

(a) (b)

Figure 5: Interface position (a) and velocity (b) for saturated R134a, considering $T_r = 0.76$.

An important aspect of the implementation of the phase-field LBM is that, in order to consider the liquid phase temperature field constant (at T_{sat}), the thermal distribution functions s_i in the liquid region were assumed to be at equilibrium with $s_i = s_i^{eq}(T_{sat})$, similarly to what was adopted by Safari *et al.* (2013). Also, the choice of the mobility parameter was the same as in Lee and Liu (2010), being $M = 0.02/\beta$. In addition, the phase-field model is not able to generate the first amount of vapor from the initial saturated liquid in contact with the superheated wall. Thus, a small vapor layer must be set on place at the beggining of the simulation. Whereas the pseudopotential method is able to generated the first amount of vapor by itself (provided the thermodynamic conditions for it).

For the evaluation of the results' accuracy, the L_2 norm error was considered. This error was defined by (Roy, 2005):

$$E_\chi^{L2} = \sqrt{\frac{\sum_{i=1}^{N} \left(\chi_i^{analit} - \chi_i^{numeric}\right)^2}{N}}\,, \tag{23}$$

where χ stands for some generic variable evaluated at N points of the domain.

The numerical results for both the interface position and velocity are presented in Fig. 2, Fig. 3, Fig. 4 (for the saturated water system), Fig. 5, Fig. 6, and Fig. 7 (for the saturated R134a). The dashed lines in these Figures represent the analytical solution presented in Sec. 3.1

By a first evaluation of the graphics in Fig. 2, Fig. 3 and Fig. 4 for water, and in Fig. 5, Fig. 6 and Fig. 7 for R134a, it is possible to observe that the phase-field model was able to recover the position and velocity of the liquid-gas interface coherently for all the three reduced temperatures simulated. On the other hand, the pseudopotential model had difficulties for recovering correctly $x_i(t)$ and $u_i(t)$ for the lowest values of TRs considered.

A more quantitative comparison between the numerical solutions can be seen in Fig. 8, where the L_2 errors are represented for each TR. For both TR$= 0.76$ and TR$= 0.86$, the errors related with the pseudopotential method are about

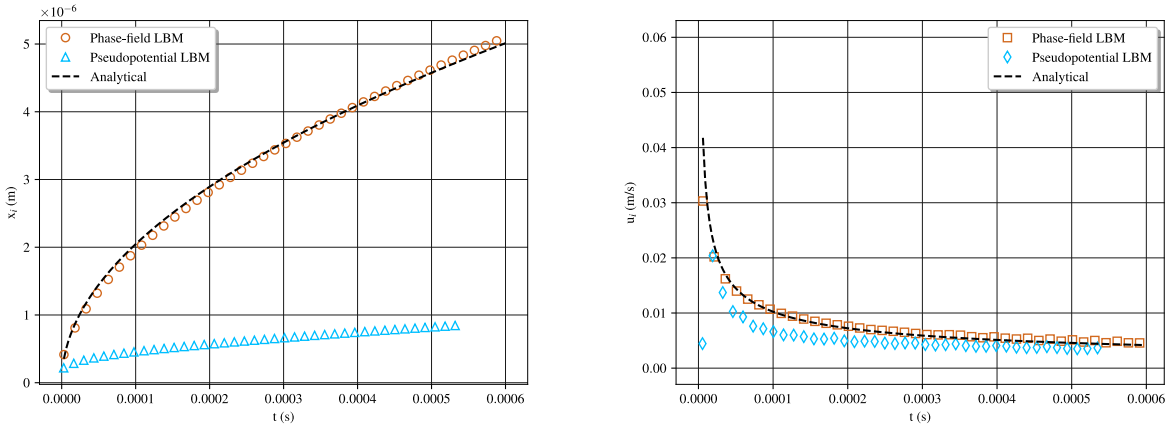

(a) (b)

Figure 6: Interface position (a) and velocity (b) for saturated R134a, considering $T_r = 0.86$.

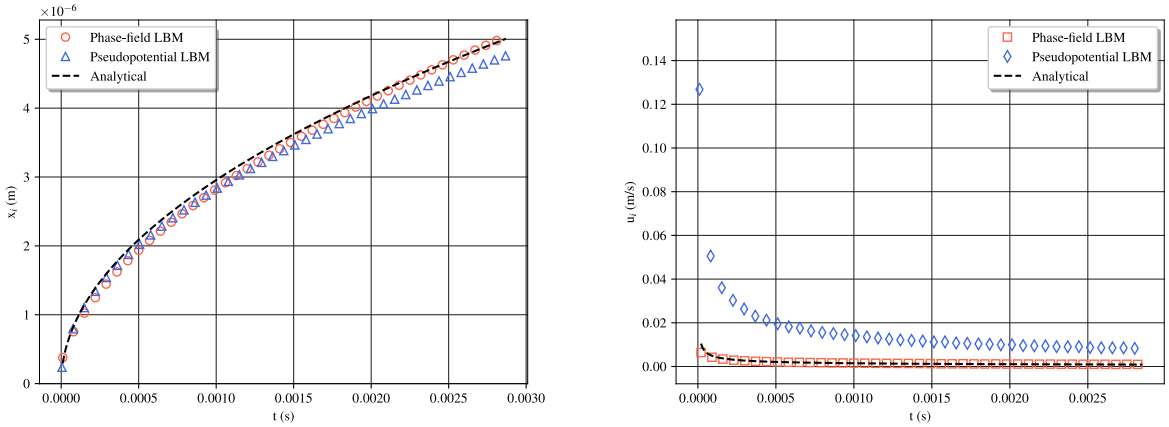

(a) (b)

Figure 7: Interface position (a) and velocity (b) for saturated R134a, considering $T_r = 0.97$.

one or even two orders of magnitude above the errors related with the phase-field model. Only at TR$= 0.97$ the errors of methods are comparable.

In summary, the errors are higher for the pseutopotential than for the phase-field model, excepting for the case of saturated water at TR$= 0.97$, where the both methods present almost the same error.

Thus, the best results were obtained when employing the Cahn-Hilliard-based phase-field LBM proposed by Lee and Liu (2010) with the Safari *et al.* (2013) modifications for considering the phase-change process. However, it is important to notice that the low values of temporal and spatial discretizations used in this paper ($\Delta t = 3.0 \cdot 10^{-11}$s and $\Delta x = 5.0 \cdot 10^{-8}$m) represent computational limitations of this LBM model (it was not possible to achieve numerical stability for higher values of Δx and Δt). This limitation was not observed for the pseudopotential model, which was able to simulate the Stefan problem with coarser discretization values. These results for the pseudopotential are not presented here since we limited our exposition to cases with the same spatial and temporal grids.

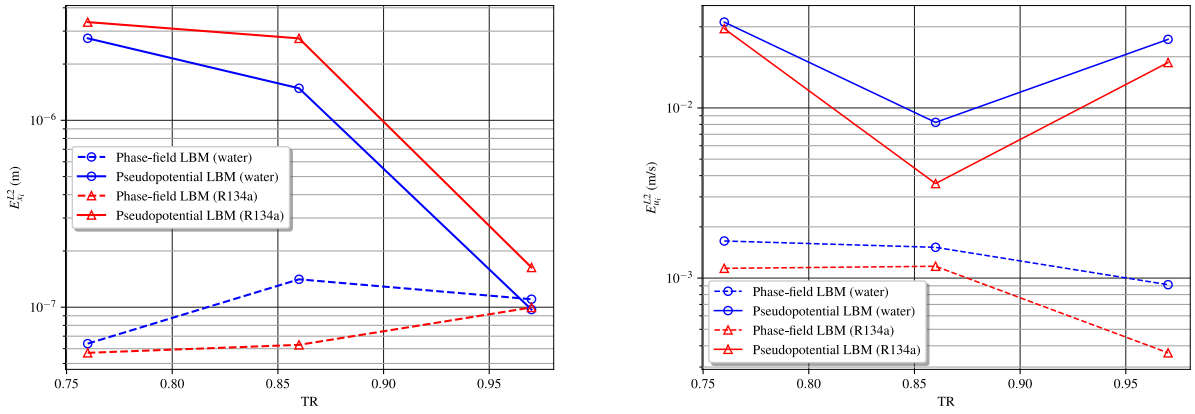

(a) (b)

Figure 8: Errors for the numerical results in comparison with the analytical solution for the interface position x_i (a) and interface speed u_i (b).

4. CONCLUSIONS

In this paper, the numerical solution of the Stefan problem was studied by the application of two different lattice Boltzmann methods for simulating phase-change processes: the pseudopotential model, and the Cahn-Hilliard-based phase-field model. It was considered two working fluids, namely water and R134a, at three reduced temperatures: 0.76, 0.86 and 0.97. The numerical results were quantitatively compared with the analytical solution of the problem in order to evaluate the performance of each model.

The results show that the Cahn-Hilliard-based phase-field model used in this work achieved the better solutions, presenting numerical results with good accuracy. However, this method suffers of stability issues, requiring to set low values for the time and space discretization parameters, Δx and Δt, decreasing the computational efficiency of the method.

Despite of presenting worse results for lower TRs, the pseudopotential method reached a reasonable accuracy for TR$=0.97$. Moreover, opposite to the phase-field model, the pseudopotential method is not so sensitive to stability issues related to Δt and Δx, allowing the use of coarser grids. An other advantage is that the pseudopotendial LBM can initialize the nucleation process, unlike the phase-field LBM.

In future studies, it is important to expand the scope of phase-change problems considered in order to conduct a more comprehensive analysis of the performance of Lattice Boltzmann Method (LBM) models. Additionally, the exploration of alternative LBM models, such as the Allen-Cahn-based phase-field models or other Cahn-Hilliard-based and pseudopotential models, would provide valuable insights. Other possibility is the inclusion of different collision operators, such as the two- or multiple-relaxation-time operators, which could enhance the understanding of the capabilities and limitations of the LBM applied to heat transfer.

5. ACKNOWLEDGEMENTS

The authors acknowledge the support received from FAPESP (São Paulo Research Foundation, grants 2023/02383-6, 2019/21022-9 and 2016/09509-1) and CNPq (National Council for Scientific and Technological Development, process 305941/2020-8).

6. REFERENCES

Bell, I.H., Wronski, J., Quoilin, S. and Lemort, V., 2014. "Pure and pseudo-pure fluid thermophysical property evaluation and the open-source thermophysical property library coolprop". *Industrial & Engineering Chemistry Research*, Vol. 53, No. 6, pp. 2498–2508.

Bhatnagar, P.L., Gross, E.P. and Krook, M., 1954. "A model for collision processes in gases. i. small amplitude processes in charged and neutral one-component systems". *Physical Review*, Vol. 94, No. 3, pp. 511–525.

Bray, A.J., 1994. "Theory of phase ordering kinetics". *Advances in Physics*, Vol. 43, No. 3, pp. 357–459.

Carey, V.P., 2020. *Liquid-Vapor Phase-Change Phenomena: An Introduction to the Thermophysics of Vaporization and Condensation Processes in Heat Transfer Equipment, Third Edition (3rd ed.)*. CRC Press.

Chapman, S. and Cowling, T.G., 1952. *The Mathematical Theory of Non-uniform Gases, 2nd ed.* Cambridge University Press.

Chen, S. and Doolen, G.D., 1998. "Lattice boltzmann method for fluid flows". *Annual Review of Fluid Mechanics*, Vol. 30, No. 1, pp. 329–364.

Fedkiw, S.O.R.P., 2003. *Level sets methods and dynamic implicit surfaces*. Springer.

Ferrari, A. and Lunati, I., 2013. "Direct numerical simulations of interface dynamics to link capillary pressure and total surface energy". *Advances in Water Resources*, Vol. 57, pp. 19–31.

Gunstensen, A.K., Rothman, D.H., Zaleski, S. and Zanetti, G., 1991. "Lattice boltzmann model of immiscible fluids". *Physical Review A*, Vol. 43, No. 8, p. 4320.

Guo, Z. and Shu, C., 2013. *Lattice Boltzmann Method and its Application in Engineering*. World Scientific Publishing Co. Pte. Ltd.

Guo, Z., Zheng, C. and Shi, B., 2002. "Discrete lattice effects on the forcing term in the lattice boltzmann method". *Physical Review E*, Vol. 65, p. 046308.

Hahn, D.W. and Özişik, M.N., 2012. *Heat Conduction, Third Edition*. John Wiley & Sons, Inc., Hoboken, New Jersey.

He, X., Chen, S. and Zhang, R., 1999. "A lattice boltzmann scheme for incompressible multiphase flow and its application in simulation of rayleigh–taylor instability". *Journal of Computational Physics*, Vol. 152, pp. 642–663.

Hirt, C.W. and Nichols, B.D., 1981. "Volume of fluid (vof) method for the dynamics of free boundaries". *Journal of Computational Physics*, Vol. 39, No. 1, pp. 201–225.

Jaramillo, A., Mapelli, V.P. and Cabezas-Gómez, L., 2022. "Pseudopotential lattice boltzmann method for boiling heat transfer: A mesh refinement procedure". *Applied Thermal Engineering*, Vol. 213, p. 118705.

Krüger, T., Kusumaatmaja, H., Kuzmin, A., Shardt, O., Silva, G. and Viggen, E., 2017. *The Lattice Boltzmann Method: Principles and Practice*. Springer Cham.

Lee, T. and Liu, L., 2010. "Lattice boltzmann simulations of micron-scale drop impact on dry surfaces". *Journal of Computational Physics*, Vol. 229, p. 8045–8063.

Li, Q., Luo, K.H. and Li, X.J., 2013. "Lattice boltzmann modeling of multiphase flows at large density ratio with an improved pseudopotential model". *Physical Review E*, Vol. 87, p. 053301.

Liu, H., Kang, Q., Leonardi, C.R., Schmieschek, S., Narváez, A., Jones, B.D., andAlbert J Valocchi, J.R.W. and Harting, J., 2016. "Multiphase lattice boltzmann simulations for porous media applications: A review". *Computer Geoscience*, Vol. 20, p. 777–805.

Lycett-Brown, D. and Luo, K.H., 2015. "Improved forcing scheme in pseudopotential lattice boltzmann methods for multiphase flow at arbitrarily high density ratios". *Physical Review E*, Vol. 91, p. 023305.

Mohamad, A.A., 2019. *Lattice Boltzmann Method: Fundamentals and Engineering Applications with Computer Codes, 2nd edition*. Springer-Verlag London Ltd.

Osher, S. and Sethian, J.A., 1988. "Fronts propagating with curvature-dependent speed: Algorithms based on hamilton-jacobi formulations". *Journal of Computational Physics*, Vol. 79, No. 1, pp. 12–49.

Premnath, K.N., McCracken, M. and Abraham, J., 2005. "A review of lattice boltzmann methods for multiphase flows relevant to engine sprays". *SAE Technical Paper Series*, Vol. 01, p. 0996.

Qian, Y.H., D'Humieres, D. and Lalleman, P., 1992. "Lattice bgk models for navier-stokes equation". *Europhysics Letters*, Vol. 17, No. 6, pp. 479–484.

Rowlinson, J.S. and Widom, B., 1982. *Molecular Theory of Capillarity*. Dover Publications, Inc.

Roy, C.J., 2005. "Review of code and solution verification procedures for computational simulation". *Journal of Computational Physics*, Vol. 205, p. 131–156.

Safari, H., Rahimian, M.H. and Krafczyk, M., 2013. "Extended lattice boltzmann method for numerical simulation of thermal phase change in two-phase fluid flow". *Physical Review E*, Vol. 88, p. 013304.

Sbragaglia, M., Benzi, R., Biferale, L., Succi, S., Sugiyama, K. and Toschi, F., 2007. "Generalized lattice boltzmann method with multirange pseudopotential". *Physical Review E*, Vol. 75, p. 026702.

Shan, X. and Chen, H., 1993. "Lattice boltzmann model for simulating flows with multiple phases and components". *Physical Review E*, Vol. 47, p. 1815.

Son, G., Ramanujapu, N. and Dhir, V.K., 2002. "Numerical simulation of bubble merger process on a single nucleation site during pool nucleate boiling". *Heat Transfer*, Vol. 124, pp. 51–62.

Swift, M.R., Orlandini, E., Osborn, W.R. and Yeomans, J.M., 1996. "Lattice boltzmann simulations of liquid-gas and binary fluid systems". *Physical Review E*, Vol. 54, No. 5, p. 5041–5052.

Welch, S.W.J. and Wilson, J., 2000. "A volume of fluid based method for fluid flows with phase change". *Journal of Computational Physics*, Vol. 160, pp. 662–682.

Zuber, N., 1959. *Hydrodynamic Apects of Boiling Heat Transfer*. Ph.D. thesis, University of California, Los Angeles, USA.

7. RESPONSIBILITY NOTICE

The authors are solely responsible for the printed material included in this paper.